



KSC Engineering Directorate
Materials Science Division

Space Spalls

STS-120 International Space Station (ISS) Starboard Solar Alpha
Rotary Joint (SARJ) Debris Analysis

Torey Salazar
M. Clara Zapata-Wright

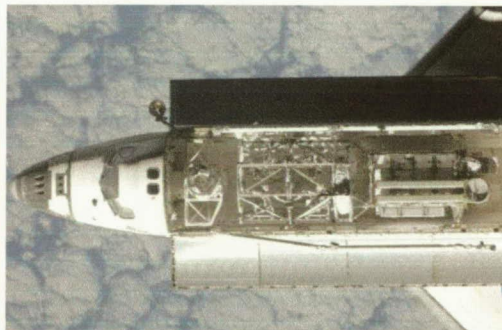
Dave Lubas
Bryan Tucker
Pete Marciniak
Phil Howard
Steve McDanelis

1



KSC Engineering Directorate
Materials Science Division

STS-117, June 2007

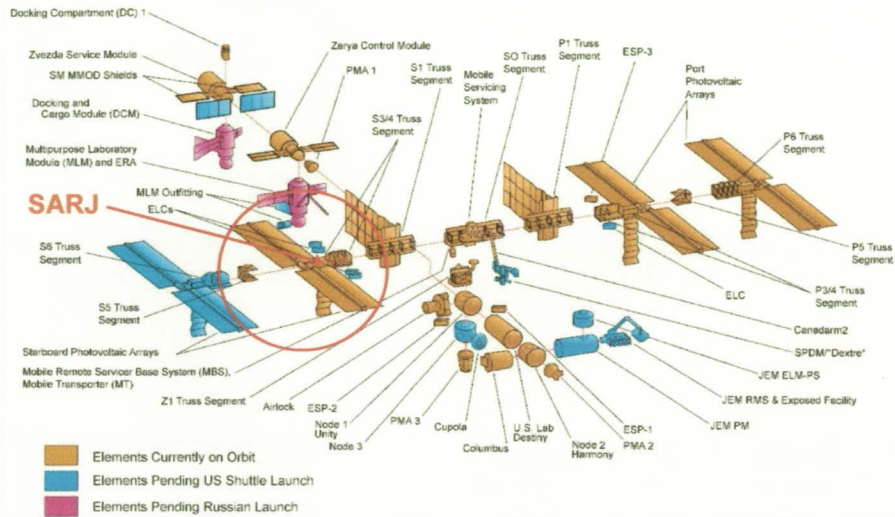


2



ISS Configuration

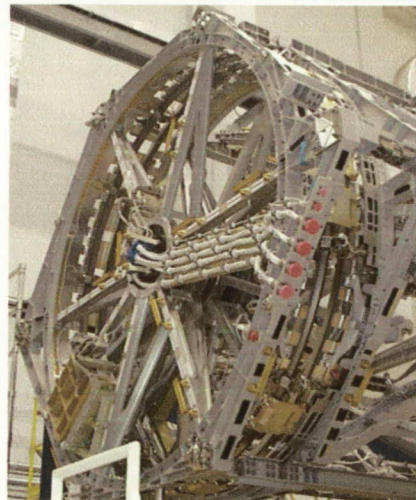
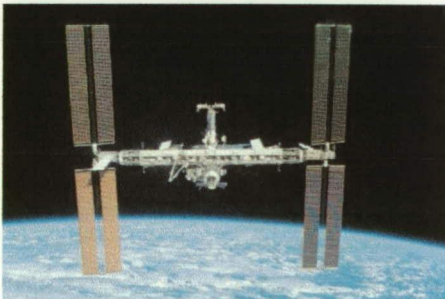
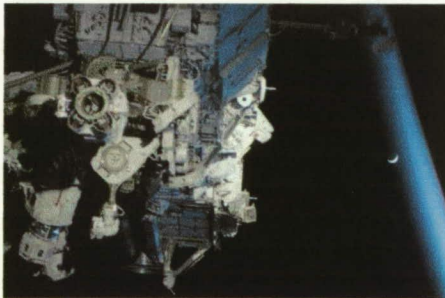
As of February 2008



3

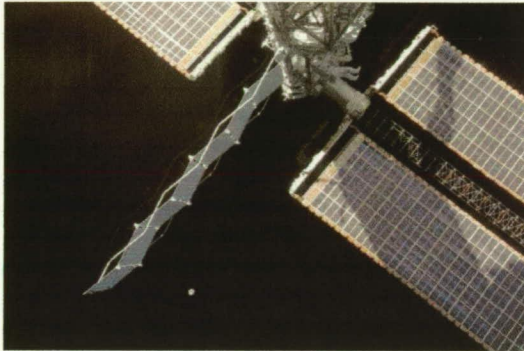


Solar Alpha Rotary Joint (SARJ)



- 10 feet in diameter.
- Rotates 360° in order to keep the solar arrays facing the sun.

4



5



- Johnson Space Center (JSC) ISS Materials & Processes (M&P) System Manager requested failure analysis of debris collected on the starboard SARJ during an extra-vehicular activity (EVA) of STS-120.
- A plan was formulated to determine the failure mechanism based on surface morphology and to determine the source of debris through elemental and particle analysis.
- The planned analysis included photodocumentation, stereomicroscopy, scanning electron microscopy (SEM), X-ray energy dispersive spectroscopy (EDS), and laser confocal microscopy.

6



- Perform photodocumentation and stereomicroscopy both before and after removing the tapes from the bag.
- Conduct baseline studies on laboratory standards of the expected SARJ mechanism alloys (Table 1), in conjunction with representative Kapton tape and Braycote grease samples.
- Perform initial SEM/EDS analysis using variable pressure and a backscattered-electron (BSE) detector to reduce charging effects and allow for the least destructive analysis.
- Remove several fragments from the tapes using a solvent and examine via SEM. Perform imaging under high vacuum and examine with secondary electrons offering higher resolution images.
- Mount and cross-section several fragments for metallographic analysis. Perform microhardness tests on the mounted fragments.
- Compare surface finish of the apparent machined surface of a large fragment with standards.

Material	UNS	C	Mn	Cr	Ni	Fe	Mo	P	S	Si	Al	Cu	Nb + Ti
Nitrided 15-5 PH	S15500	0.07 max	1.0 max	14-15.5	3.5-5.5	bal		0.04 max	0.03 max	1.0 max		2.5-4.5	0.15-4.5
440C	S44004	0.95-1.20	1.0 max	16-18		bal	0.75 max	0.04 max	0.03 max	1.0 max			
13-8Mo	S13800	0.05 max	0.1 max	12.25-13.25	7.50-8.50	bal	2.0-2.5	0.01 max	0.008 max	0.1 max	0.9-1.35		
17-7 PH	S17700	0.09 max	1.0 max	16-18	6.5-7.75	bal		0.04 max	0.03 max	1.0 max	0.75-1.5		

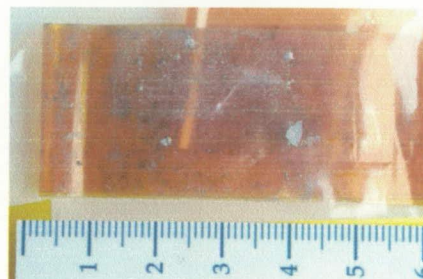
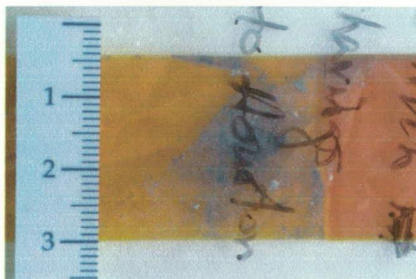
Table 1 Potential Debris Compositions, %a. Highlighted boxes indicate the constituents that vary significantly between the expected alloys in the SARJ.

Source: ASM Handbook Vol. 1

7



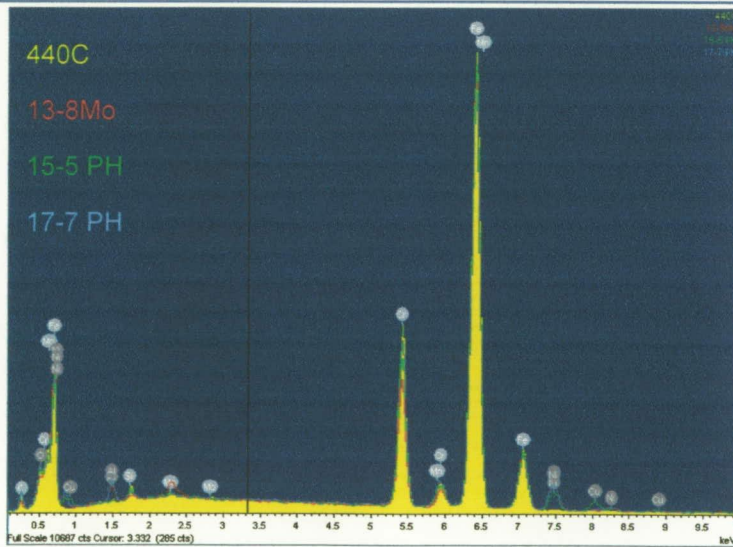
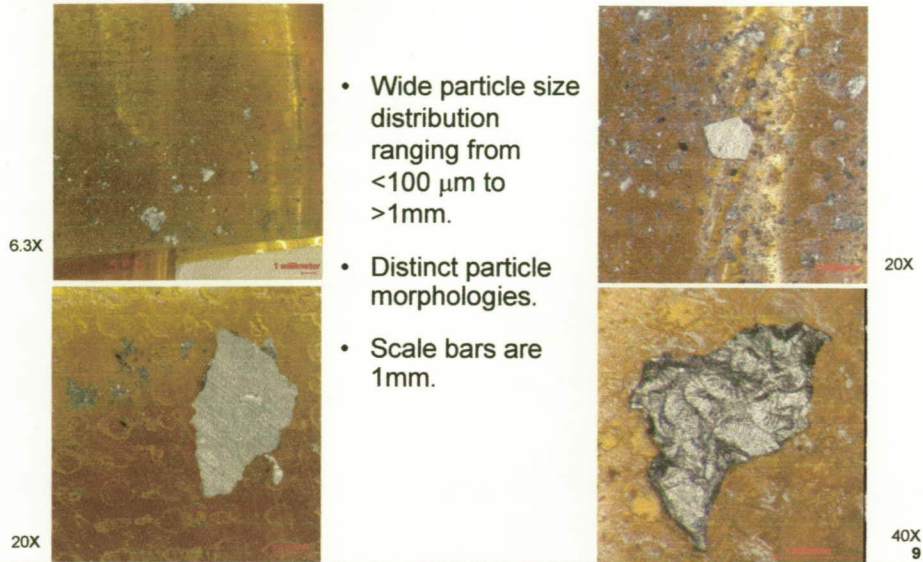
- Following landing and de-stow, Boeing KSC M&P delivered the samples to the Materials Failure Analysis Laboratory.
- Three sample tapes were received for analysis and were photographed, as-received.



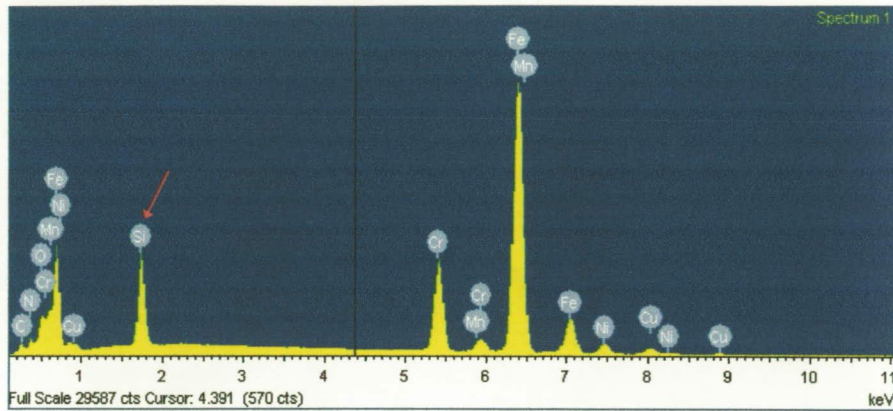
8



Representative particles from the tapes.

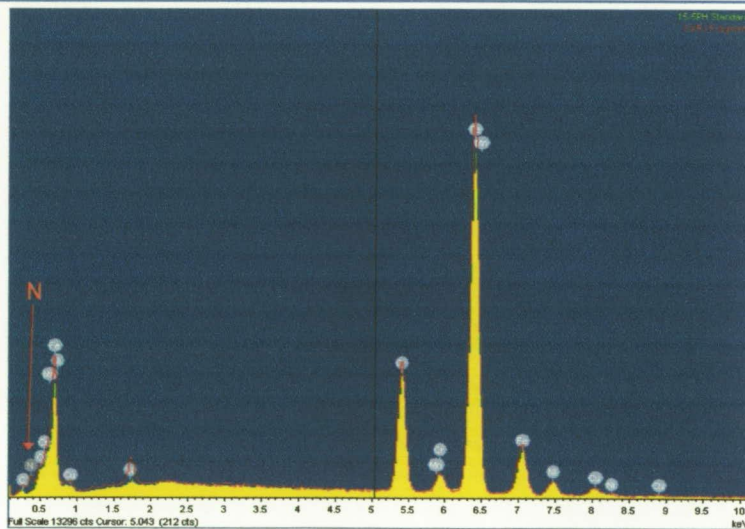


Spectra of the standards from expected SARJ alloys (Table 1, slide 7) are shown overlayed to display the differences in constituents.



Representative spectrum from debris – corresponds most closely to nitrided 15-5 PH. The silicon peak is due to the silicone adhesive on the Kapton tape.

11

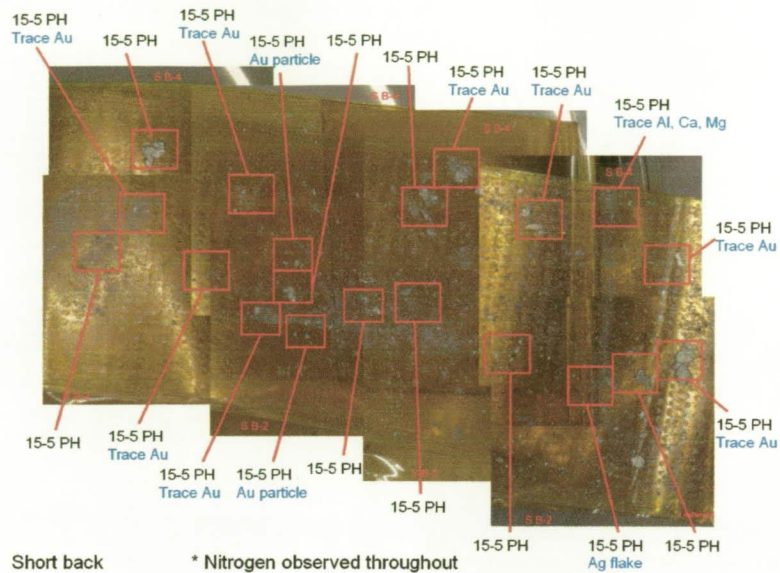


Overlay of representative spectrum from debris (red) on the baseline 15-5 PH spectrum. N peak indicates that the debris is from the nitrided layer.

12



Chemical Analysis of Short Back Sample



13

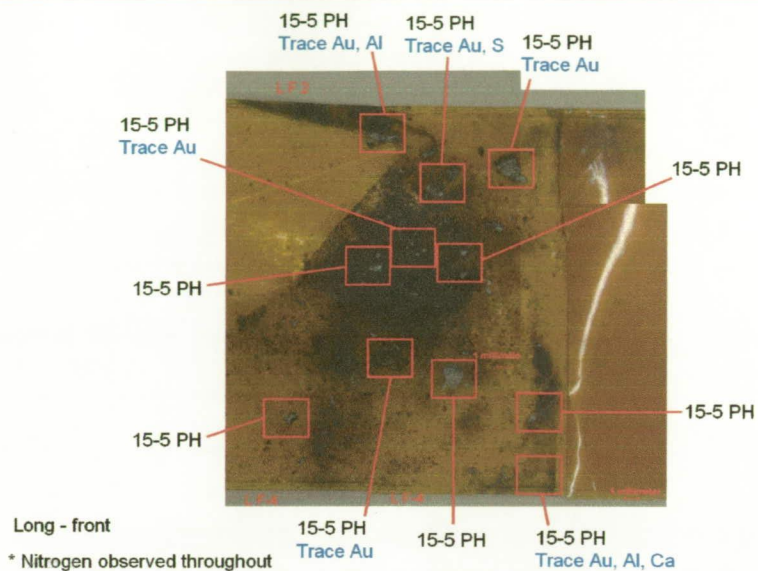


Chemical Analysis of Short Front Sample



14

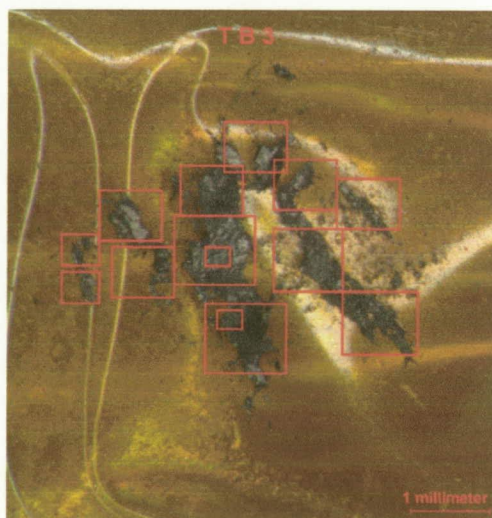
Chemical Analysis of Long Front Sample



15

Chemical Analysis of Third Back Sample

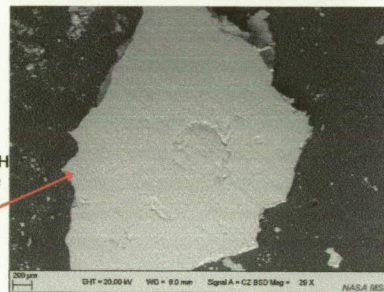
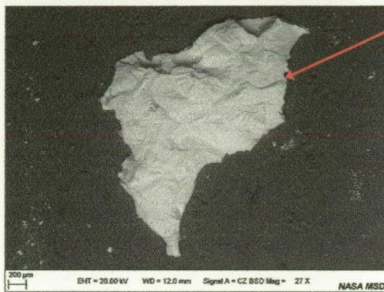
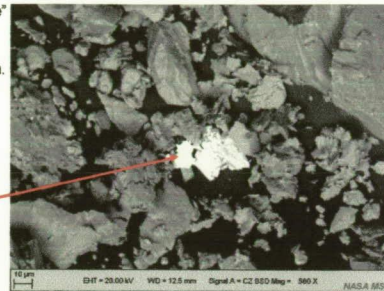
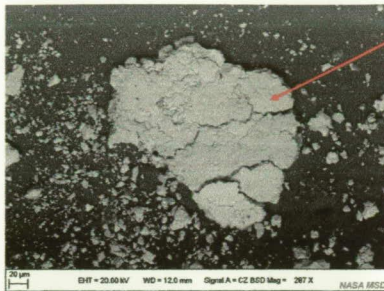
All 15-5 PH with Nitrogen
No trace elements



16



SEM Images of Short sample

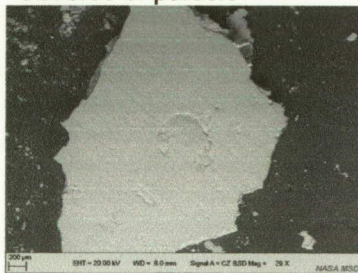


17



SEM Images of Large Particle from Short Front Sample

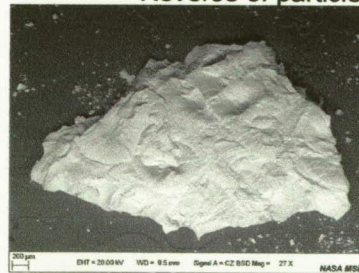
Obverse of particle



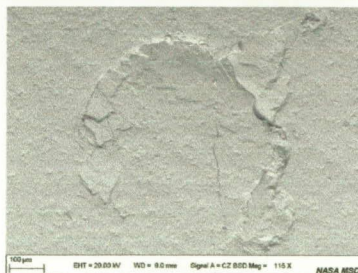
Flipped and rotated



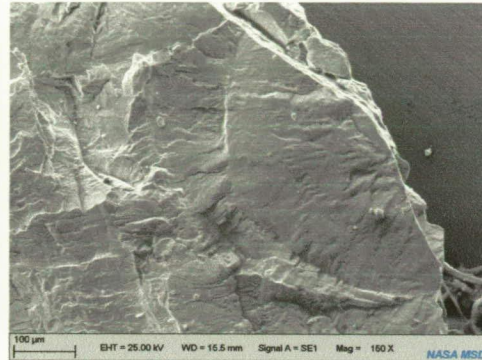
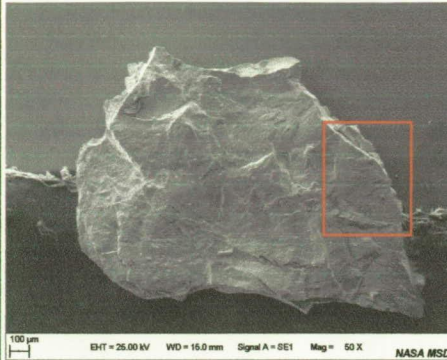
Reverse of particle



Nitrided 15-5 PH surface with machine markings on obverse (L) and flipped over revealing scalloped reverse (R).

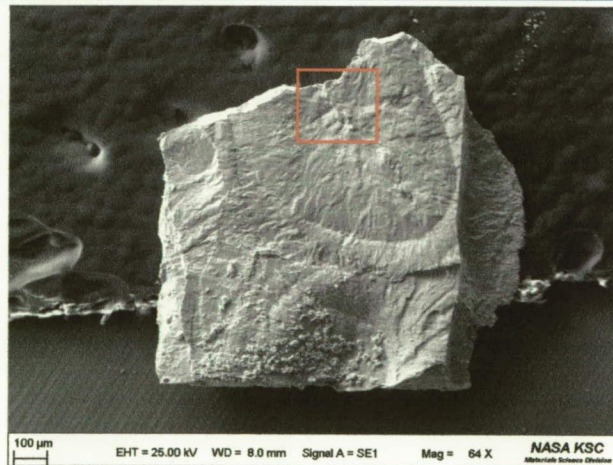


18



SEM image of fragment removed from tape imaged under high vacuum in secondary electron (SE) mode. Area in red box appears to be a fracture initiation site and fan-shaped region within the box suggests crack arresting.

19

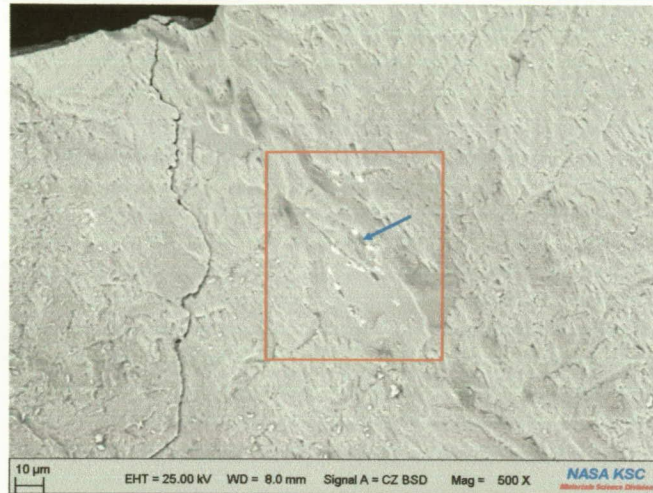


SEM image of fragment removed from tape and imaged under high vacuum in secondary electron (SE) mode. Area in red box appears to be a fracture initiation site and elliptical region suggests crack arresting. Features typical of spalled fragments.

20



Backscattered Electron Image of an Initiation Site

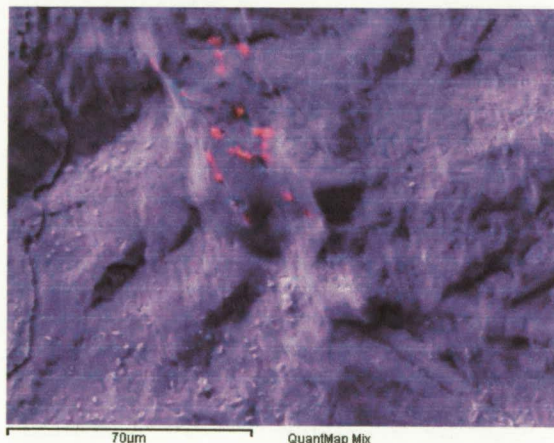


Backscattered electron image of outlined area in red box from slide 21 showing atomic contrast. The white constituent in the box is primarily niobium (Nb), and the black constituent next to the blue arrow is MnS, as confirmed by EDS.

21



X-Ray Elemental Dot Map at Initiation Site



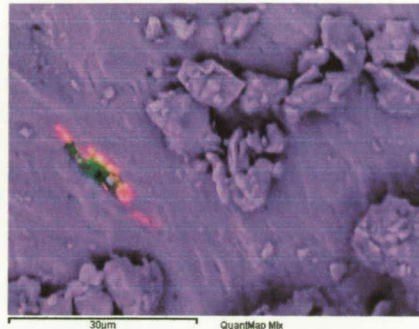
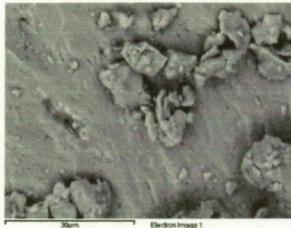
Violet = Fe
Red = Nb
Green = Mn
Aqua = S

X-ray elemental dot map of same apparent initiation site outlined in slide 21, showing Nb-rich precipitates in an Fe-rich matrix. Note: Mn and S pixels are masked in this image.

22



X-Ray Elemental Dot Map



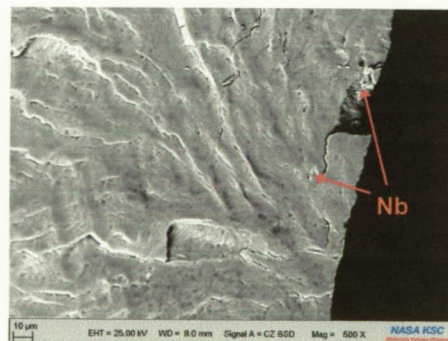
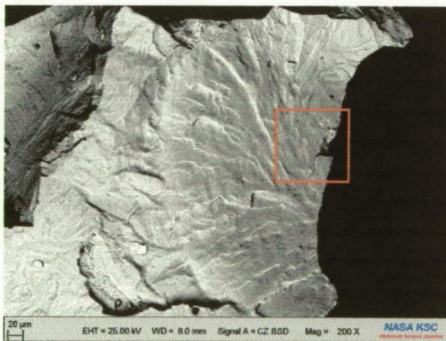
Violet = Fe
Red = Nb
Green = Mn
Aqua = S

X-ray elemental dot map showing Nb-rich precipitates in an Fe-rich matrix and a MnS inclusion. MnS inclusions were often located in the vicinity of the Nb-rich precipitates.

23



Additional Fracture Initiation Sites with Nb-Rich Precipitates

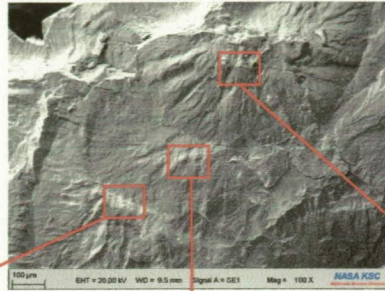


Backscattered electron image showing atomic contrast of the Nb-rich precipitates at a typical subsurface fracture initiation site.

24



Additional Fracture Initiation Sites with Nb-Rich Precipitates



Backscattered electron image showing atomic contrast of the Nb-rich precipitates at typical subsurface fracture initiation sites.

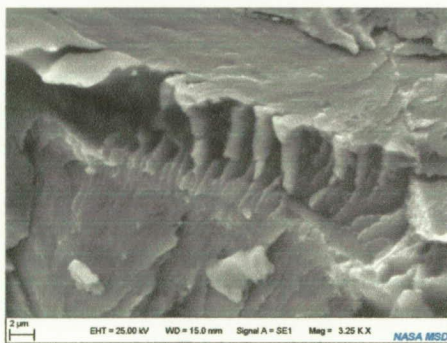


25



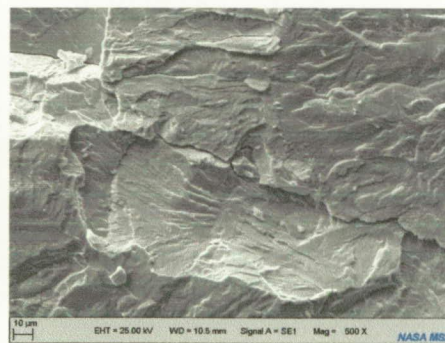
Typical Brittle Fracture Features

Side of fragment



Cleavage steps

Reverse face of fragment



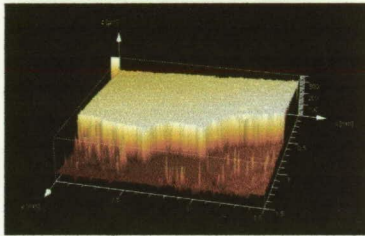
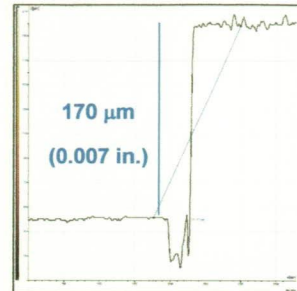
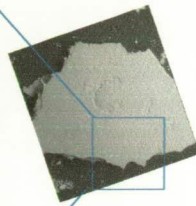
Cleavage feather pattern

26



Confocal Microscopy for Particle Thickness

Typical confocal topographical images (2D, 3D) and resulting chart.

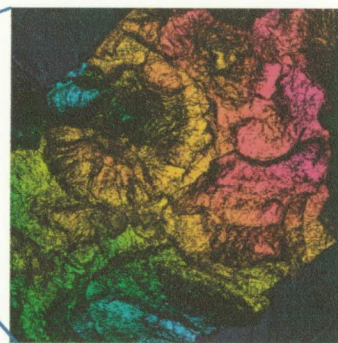
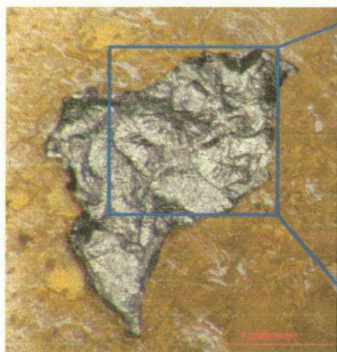


- Confocal microscopy was used for in-situ (non-destructive) thickness measurements at 100X magnification of several particles.
- Particle thickness ranged from 100 to 260 μm , however minor margin of error may exist from the possibility of particles lifting off tape or being imbedded into tape.

27

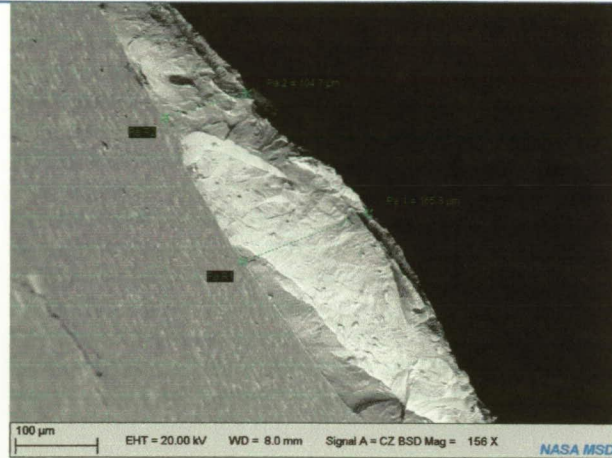


Confocal Microscopy for Surface Topography



Confocal microscopy was used to study the relative heights on the fragment fracture surface. Image on right shows the topography using the visible spectrum, with the highest areas in red/pink and the lowest areas in dark blue (background).

28

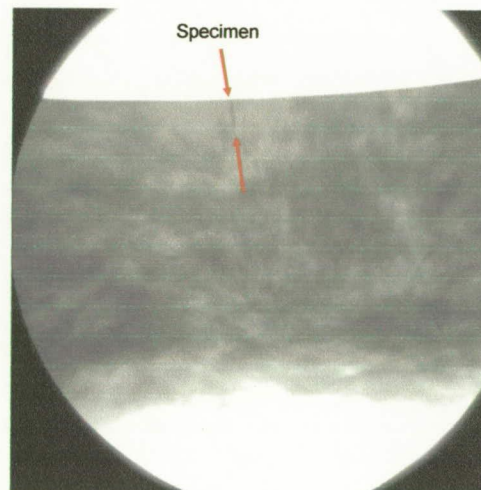


Particle thickness measurements of large particle in the SEM correlated with measurements taken using laser confocal microscopy, which were 100 to 165 μm for this particle.

29



- Two larger fragments were hot mounted in conductive epoxy resin.
- One large fragment was cold mounted in a two-part resin.
- A nitrided 17-4 PH bull gear exemplar was prepared for methodology and microstructure comparison.
- Specimens were ground, polished, and etched to examine the cross sectional microstructure.
- Real-time X-ray was utilized to locate the specimen in the metallographic mount and provide orientation and progress during polishing (right).



30



Exemplar
nitrided 17-4 PH
bull gear cross
section.

500X



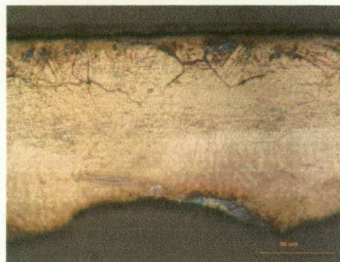
Nitrided case (0.0046")

Interface

Martensitic core

SARJ nitrided
15-5 PH
fragment cross
section.

500X



No martensitic core was
observed in SARJ
fragment.

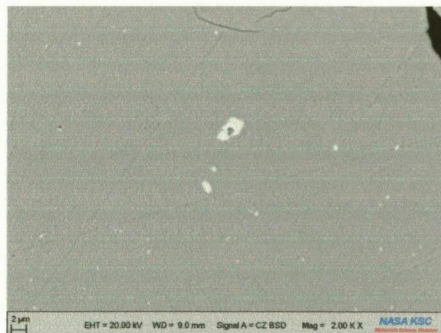
Etchant: Fry's Reagent

31



SARJ fragment

Stock 15-5PH



Backscattered electron image showing atomic contrast of typical Nb-rich precipitates (white) and MnS inclusions (black) in the 15-5 PH matrix (gray). The geometry and length scale of the SARJ fragment precipitates were comparable with those of stock 15-5 PH. The hardness of the stock 15-5 PH indicated that it has a similar heat treatment as the SARJ specification.

32



- Knoop microhardness testing with 100 gram load.
- Microhardness of the mounted cross section was approximately 996 HK 100.
- Extrapolated converted microhardness of the mounted cross section was approximately 71 Rockwell C scale (HRC).

33



- Predominantly two types of chips were present on the tape: a fine debris and larger fragments that displayed fracture features.
- Energy dispersive X-ray spectrometry (EDS) indicated that the majority of the chips were 15-5 PH nitrided stainless steel.
- No apparent 15-5 PH substrate was observed.
- Distinct gold flakes and trace gold was observed at various locations throughout the debris.
- Thicknesses of the large fragments have been within the thickness of the nitrided layer.

34

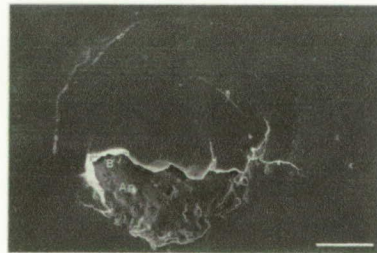


- Based upon morphology, the majority of the fine debris consistently displayed mechanical damage.
 - The fine debris displayed “extrusion-like” damage, a result of severe plastic deformation imparted during excessive metal distress, obliterating and obscuring any original fracture features.
 - Agglomeration of various chips was observed.
- The largest fragment that exhibited a possible machined surface on its obverse was turned over and displayed mechanical damage, similar to scalloping, on its reverse.
- Metallography performed on three larger fragments indicated that the fragmentation was limited to the nitrided case layer.
- Converted microhardness measurements were consistent with the mechanical properties of a nitrided case layer.

35



- Contact stress fatigue, i.e. spalling, with subsurface initiation
 - Location of origin – “Short distance below surface, usually at a nonmetallic inclusion”
 - Initial size – “Small”
 - Initial shape – “Irregular”
 - Crack angle with respect to surface – “Roughly parallel at bottom, perpendicular at sides”
 - Apparent occurrence – “Sudden”



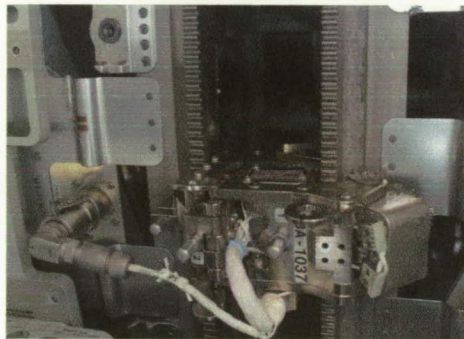
* Wulpi, D.J., *Understanding How Components Fail*. ASM International. 1985. p. 199.

36



KSC Engineering Directorate
Materials Science Division

Expedition 16, EVA 13, December 2007



37



KSC Engineering Directorate
Materials Science Division

STS-122 (February 2008) and
STS-123 (March 2008)



38